NMR Quantification of Halogen-Bonding Ability to Evaluate Catalyst Activity

Yun-Pu Chang, Teresa Tang, Jake R. Jagannathan, Nadia Hirbawi, Shaoming Sun, Jonah Brown, Annaliese K. Franz*

Department of Chemistry, University of California, One Shields Avenue, Davis, California 95616, United States

Supporting Information Placeholder

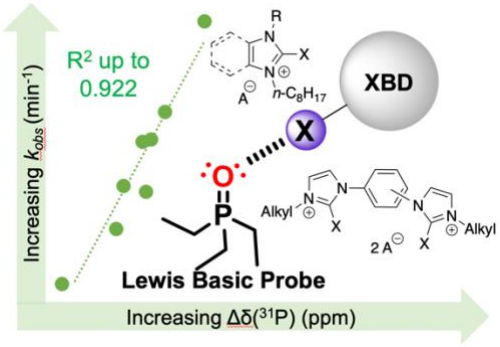

ABSTRACT: Quantification of halogen-bonding abilities is described for a series of monodentate and bis(imidazolium) halogen-bond donors (XBDs) using ^{31}P NMR spectroscopy. The measured Δδ(^{31}P) values correlate with calculated activation free energy ΔG‡ and catalytic activity for a Friedel–Crafts indole addition. This rapid method also serves as a sensitive indicator for Brønsted acid impurities.

Halogen-bonding (X-bonding) is a noncovalent interaction between an electrophilic halogen atom and a Lewis base.[1] Owing to the high directionality, hydrophobicity, and tunability, X-bonding has been utilized in crystal engineering and material science to control molecular assembly.[2,3] More recently, X-bonding has been applied to molecular recognition[4] and catalysis[5] in solution-phase.[6] In general, X-bonding of organic scaffolds is a relatively weak interaction with a low association affinity to Lewis bases.[7] The investigation of X-bonding on organic scaffolds relies on high sensitivity techniques such as IR,[8] Raman,[9] UV–Vis,[10] and NMR[11-13] spectroscopies.

Due to the versatility and ability to provide detailed structural information, solution NMR spectroscopy has been the most common technique for analyzing X-bonding for organic scaffolds (Figure 1).[11] With ^{1}H and ^{19}F NMR, chemical shifts provide insight regarding X-bonding at least two bonds away from the interaction site to the reporter nucleus, albeit often with low magnitudes of the detectable signal (Figure 1A).[5f, 11b–c] Examples of ^{13}C NMR spectroscopy have been successfully used to detect the formation of X-bonding in solution, yet the intrinsic low abundance limits the sensitivity, decreasing the applicability to quantify X-bonding (Figure 1B).[5j, 12] Several examples of quantification of X-bonding using ^{15}N NMR spectroscopy have been reported;[13] however, even though the reporter nitrogen is directly interacting with the halogen atom, the author reported that the evaluation of weak X-bonding interactions is not sufficiently accurate (Figure 1C).

^{31}P NMR spectroscopy has been successfully applied to quantify noncovalent interactions upon binding to triethylphosphine oxide (TEPO) as a Lewis basic probe.[14–16] First reported by Gutmann and Beckett to measure Lewis acidic solvents,[14] we and others have since adapted this method to quantify the H-bonding ability of various H-bond donors.[15] Previous work in our group has successfully demonstrated the proportional relationship of H-bonding ability and catalytic activity for a variety of H-bonding donors using ^{31}P NMR spectroscopy (Figure 1D).[16]

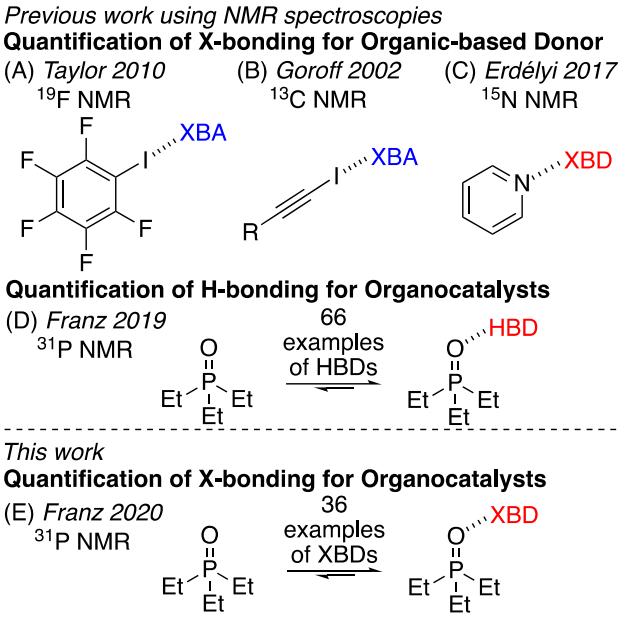

Figure 1. Quantification of noncovalent interactions using NMR spectroscopy.

Compared to the extensive application for H-bonding, the investigation of X-bonding ability for organocatalysts is limited.[5j, 17] Here, we report using ^{31}P NMR spectroscopy method to systematically quantify X-bonding ability and correlate the catalytic ability for XBD organocatalysts (Figure 1E). This work examines representative XBD compounds including neutral (**1**-**4**), cationic benzimidazolium- (**5**),[5e, 5f] imidazolium- (**6**-**7**),[5e–f, 5i] and bis(imidazolium)-based[5e, 5g] (**8**-**9**) structures (Figure 2).

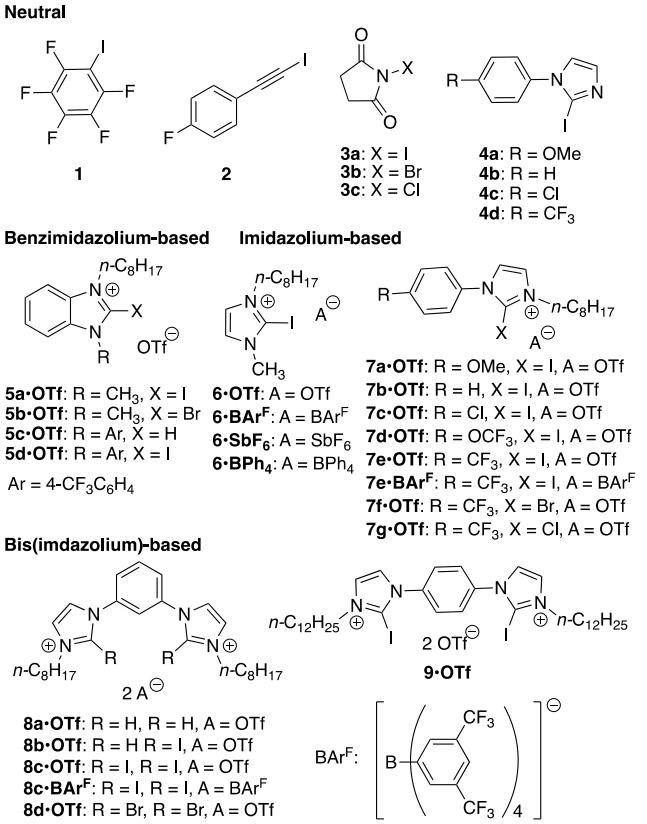

Figure 2. Halogen-bond donors studied.

Method Validation To validate ^{31}P NMR spectroscopy as a method to quantify X-bonding ability, factors such as the XBD−TEPO equilibrium, solvent interferences and the competition of other noncovalent interactions from impurities were carefully examined.[18] Downfield ^{31}P NMR shifts (Δδ) are observed upon TEPO binding to XBDs (Figure 3A).[19] Stronger X-bonding ability is expected to correlate to larger Δδ(^{31}P) values. To assess the XBD−TEPO binding equilibrium,[20] titration experiments of XBD (relative to TEPO) were investigated (Figure 3B). For imidazolium- (**6•OTf**) and bis(imidazolium)-based triflate (**8c•OTf**) XBDs, saturation occurs at approximately 10 and 15 equivalents, respectively. With the weakly coordinating counteranion, **7e•BAr^F** and **8c•BAr^F** XBDs possess enhanced binding ability[21] and saturation was observed for each at ~5 equivalents.

To assess that TEPO binding can probe X-bonding ability, the Δδ(^{31}P) values for XBDs with different electrophilic halogen atoms were measured (Figure 2, **5a–5b•OTf**, **7e–7g•OTf**, **8c–8d•OTf**). The more electrophilic halogen atom (I > Br > Cl) should correlate with larger Δδ(^{31}P) values. Indeed, switching from iodo to bromo and chloro (in **7e-7g•OTf**) significantly decreased Δδ(^{31}P) values (Table 1), matching a decrease in polarizability of the halogen substituents and hence the X-bonding ability.

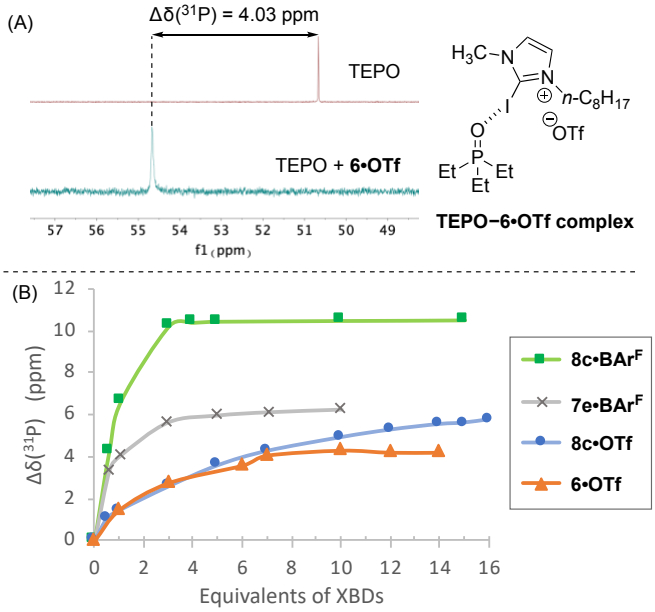

Figure 3. (A) Example ^{31}P NMR spectra for the downfield ^{31}P NMR shifts upon TEPO binding to XBD (in CD_2Cl_2). (B) Titration experiments comparing XBDs. Calculation of binding constant: **8c•BAr^F**, K_a = 186 ± 4 M^{-1} (see SI).[21]

To validate ^{31}P NMR spectroscopy and the ability of TEPO binding to quantify electronic effects for X-bonding, a Hammett plot was created for a series of 2-iodoimidazolium triflate salts (**7a−7e•OTf**) with electronically varied substituents on the conjugated benzene ring (Table 1, Figure 4). A linear relationship (R^2 = 0.988) was observed, indicating that Δδ(^{31}P) values can accurately quantify the electronic changes affecting X-bonding ability.

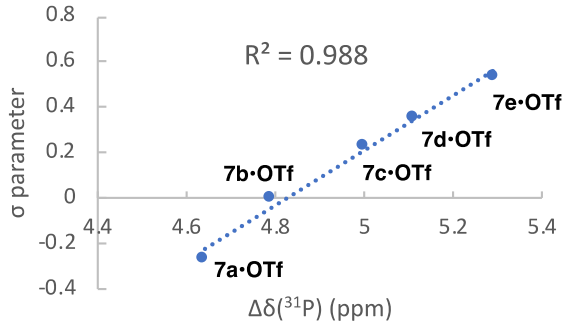

Figure 4. Correlation of Δδ(^{31}P) and Hammett σ parameters for imidazolium triflates **7a−7e•OTf** (Table 1).

Result and Discussion To build a scale to quantify X-bonding ability of organocatalysts, Δδ(^{31}P) values were measured for a variety of XBD compounds (Table 1). TEPO binding with most neutral XBDs (e.g. **1−2**, **4**) results in very low Δδ(^{31}P) values, indicating low X-bonding ability; however, X-bonding ability were notably increased with a high electronegative atom attached to the halogen atom (e.g. **3a**). Without the cationic charge on the XBD core, the Δδ(^{31}P) values are < 1.0 ppm and interactions are too weak to observe trends, highlighting the importance of the cationic charge for increasing the X-bonding ability (e.g. **4a−4d**). The larger Δδ(^{31}P) value of cationic benzimidazolium-based XBD (**5a•OTf**, Δδ(^{31}P) = 4.94 ppm) compared to cationic imidazolium-based XBD (**6•OTf**, Δδ(^{31}P) = 4.03 ppm) suggested higher X-bonding ability. This is

attributed to the extended aromaticity of the benzimidazolium core.[22] By increasing the electron deficiency of the benzimidazolium core (**5d•OTf**), the largest $\Delta\delta(^{31}P)$ value among cationic XBD triflates was observed (5.76 ppm).

^{31}P NMR spectroscopy was also utilized to investigate the effect of different counteranions for imidazolium **6** on X-bonding interactions.[5e, 5h] The largest $\Delta\delta(^{31}P)$ value was measured for **6•BAr^F** (5.68 ppm) matching the decreased coordinating ability for the BAr^{F-} counterion and hence increased X-bonding ability. The $\Delta\delta(^{31}P)$ values for **6•SbF$_6$** and **6•BPh$_4$** were observed to generally follow the trend for anion-coordinating ability.[23, 24]

Table 1. Measured ^{31}P NMR shifts and k_{obs} for XBDs in CD_2Cl_2

XBD[a]	$\Delta\delta(^{31}P)$ (ppm) Trial 1[b]	$\Delta\delta(^{31}P)$ (ppm) Trial 2[b]	$\Delta\delta(^{31}P)$ (ppm) Trial 3[b]	Avg $\Delta\delta(^{31}P)$ (ppm)[c]	$k_{obs} \times 10^{-4}$ min^{-1}
1	0.20	0.22	0.22	0.21	NR[d]
2	0.12	0.14	0.13	0.13	-
3a	10.01	9.99	9.97	9.99	-[e]
3b	1.42	1.36	1.44	1.41	-[e]
3c	1.34	1.41	1.38	1.38	-
4a	0.05	0.01	0.05	0.04	-
4b	0.84	0.82	0.84	0.83	-
4c	0.89	0.89	0.97	0.92	-
4d	0.88	0.89	0.89	0.89	-
5a•OTf	4.94	4.94	4.93	4.94	4.57
5b•OTf	1.77	1.64	1.61	1.67	-
5c•OTf	1.24	1.26	1.25	1.25	-
5d•OTf	5.77	5.74	5.76	5.76	13.00
6•OTf	4.06	4.02	4.01	4.03	NR[d]
6•BAr^F	5.75	5.65	5.66	5.68	5.77
6•SbF$_6$[f]	5.34	5.29	5.29	5.31	-[g]
6•BPh$_4$[f]	4.62	4.49	4.46	4.52	-[g]
7a•OTf	4.70	4.68	4.68	4.69	2.72
7b•OTf	4.79	4.78	4.78	4.78	4.86
7c•OTf	5.00	5.01	5.01	5.01	7.03
7d•OTf	5.12	5.10	5.11	5.11	7.16
7e•OTf	5.29	5.28	5.29	5.28	8.51
7e•BAr^F	6.24	6.29	6.23	6.25	11.47
7f•OTf	1.43	1.44	1.39	1.42	NR[d]
7g•OTf	1.22	1.13	1.27	1.21	NR[d]
8a•OTf[h]	0.94	0.99	0.98	0.97	NR[d]
8b•OTf[h]	4.87	4.88	4.88	4.88	8.23
8c•OTf[h]	4.91	4.92	5.03	4.95	9.21
8c•BAr^F[i]	10.47	10.44	10.46	10.46	32.64
8d•OTf[h]	2.54	2.46	2.52	2.51	NR[d]
9•OTf[j]	4.01	3.90	3.89	3.91	8.28

[a]Experiments performed at 15 mM TEPO in CD_2Cl_2 with 10 equiv XBD unless otherwise indicated. [b]$\Delta\delta(^{31}P)$ = δ(XBD•TEPO complex) – δ(free TEPO) [c]Standard deviation (n=3) for all XBDs are <0.10 ppm. Avg $\Delta\delta(^{31}P)$ values used for correlation. [d]No reaction observed; k_{obs} assumed to be zero. [e]Not reported; observed rate is attributed to *in-situ* formation of elemental halogens (e.g. I_2) rather than respective XBDs. [f]One drop of 2,6-di-*tert*-butylpyridine (DTP) was added. [g]No reaction observed with DTP added. [h]Using 15 equiv of XBD. [i]Using 5 equiv of XBD. [j]Using 3 equiv of XBD.[26]

To investigate the denticity effect based on substituent pattern for X-bonding ability, bis(imidazolium) salts **8-9** were quantified. $\Delta\delta(^{31}P)$ values were collected using 3.0 equivalents of XBD (relative to TEPO) for the direct comparison between meta-substituted **8c•OTf** (2.58 ppm) and para-substituted bis(imidazolium) **9•OTf** (3.91 ppm).[26] The larger $\Delta\delta(^{31}P)$ value of **9•OTf** suggests enhanced bidentate capability for the para-substituted bis(imidazolium); however, it was observed that meta-substituted bis(imidazolium) **8c•BAr^F**, has a nearly double $\Delta\delta(^{31}P)$ relative to **6•BAr^F**, suggesting bidenticity with the **BAr^F** counterion.[25]

TEPO Signal as an Indicator for Impurities An integral part of this quantification method is to ensure the absence of any impurities, especially trace acids formed from the counter-anions. Impurities that bind with the TEPO probe effectively can broaden and shift the ^{31}P NMR signal (e.g. Figure 5A vs 5B). Undesired $\Delta\delta(^{31}P)$ values from broad peaks would not accurately reflect the X-bonding ability (i.e. Figure 5B). To remove acid (and other) impurities, a purification procedure was performed for XBDs and the ^{31}P NMR signals were compared before and after purification.[27] A sharp peak and reliable $\Delta\delta(^{31}P)$ values were consistently acquired when purified XBDs were used in binding experiments (Figure 5A). Even in cases when ^1H and ^{19}F NMR did not detect impurities, the ^{31}P NMR signal was shown to be more sensitive. Therefore, it is noteworthy that ^{31}P NMR and the TEPO signal can serve as a sensitive indicator for trace amounts of impurities that may not be detectable using ^1H and ^{19}F NMR (see Supporting Information, Section VIb).

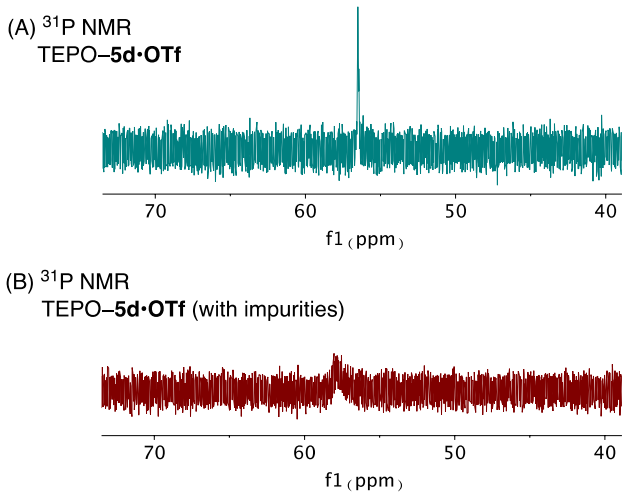

Figure 5. (A) Reliable and consistent $\Delta\delta(^{31}P)$ values are determined from sharp ^{31}P NMR signals after rigorous purification (e.g. binding to **5d•OTf**). (B) Even when no TfOH is observed using ^1H and ^{19}F NMR, a broader peak is observed using ^{31}P NMR (after extraction and the first silica column).[27]

Correlation of $\Delta\delta(^{31}P)$ and $\Delta G^{\ddagger}$ The ability to correlate ^{31}P NMR data with thermodynamic properties was envisioned by using activation free energy $\Delta G^{\ddagger}$ values for reactions catalyzed by XBDs. Measured $\Delta\delta(^{31}P)$ values were compared to previously calculated $\Delta G^{\ddagger}$ values[28] for a Friedel–Crafts addition of indole **10** to *trans*-crotonophenone **11** catalyzed by XBD organocatalysts in benzene (Eq 1). The direct comparison between $\Delta\delta(^{31}P)$ and calculated $\Delta G^{\ddagger}$ values affords a good correlation (R^2 = 0.775). Considering the logarithm form of Arrhenius equation, log $\Delta\delta(^{31}P)$ values were also examined and show a stronger correlation with $\Delta G^{\ddagger}$ (R^2 = 0.899). The strong

correlation between log $\Delta\delta(^{31}P)$ and calculated $\Delta G^{\ddagger}$ values demonstrates the capability of correlating ^{31}P NMR shifts with thermodynamic properties. The data also suggest that TEPO is a suitable isostere for carbonyl activation-type reactions.

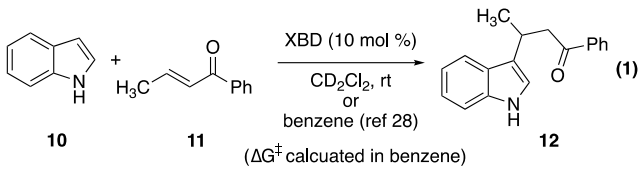

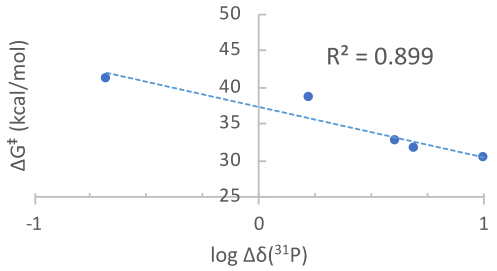

XBD	$\Delta\delta(^{31}P)$ (ppm)	*ln* $\Delta\delta(^{31}P)$	*log* $\Delta\delta(^{31}P)$	$\Delta G^{\ddagger}$ (kcal/mol)[a]
1	0.21	-1.56	-0.68	+41.0
5b•OTf	1.67	0.51	0.22	+38.3
6•OTf	4.03	1.39	0.61	+32.5
5a•OTf	4.94	1.60	0.69	+31.5
3a	9.99	2.30	1.00	+30.3

[a]Calculated activation free energies were obtained from ref. 28

Figure 6. Correlation ($R^2 = 0.899$) of calculated $\Delta G^{\ddagger}$ values (in benzene)[28] for the Friedel-Crafts reaction of indole **10** to *trans*-crotonophenone **11** with log $\Delta\delta(^{31}P)$ values (in CD_2Cl_2).

Correlation of Δδ(³¹P) and Catalytic Activity The measured $\Delta\delta(^{31}P)$ values for XBDs were correlated to catalytic activity for a Friedel–Crafts indole addition (Eq 1 and Figure 7A).[28–30] In order to evaluate using ^{31}P NMR spectroscopy to predict catalytic activity, the observed rates (k_{obs}) of the Friedel–Crafts addition reaction in CD_2Cl_2 were monitored using ^{1}H NMR spectroscopy (Table 1; see details in Supporting Information).[31] Based on the observed correlation, when $\Delta\delta(^{31}P)$ is less than 4.03 ppm, the X-bonding interaction is too weak to promote the indole addition (Table 1). The XBD with highest catalytic activity, bisimidazolium BAr^F salt (**8c•BAr^F**), was successfully predicted by the largest $\Delta\delta(^{31}P)$ value (10.46 ppm). Moreover, a linear relationship was observed for Hammett σ parameters to the rate constants k_{obs} for para-substituted phenyl-imidazolium triflate XBDs (Table 1, **7a–7e•OTf)** (Figure 7B). While the overall correlation for XBDs studied was lower ($R^2 = 0.765$), a high correlation is observed between $\Delta\delta(^{31}P)$ values and k_{obs} within the sub-class of monodentate triflate XBDs ($R^2 = 0.922$). This correlation supports that TEPO binding and $\Delta\delta(^{31}P)$ values can be a predictor of catalytic activity for carbonyl activation-type reactions within structural classes of XBDs.

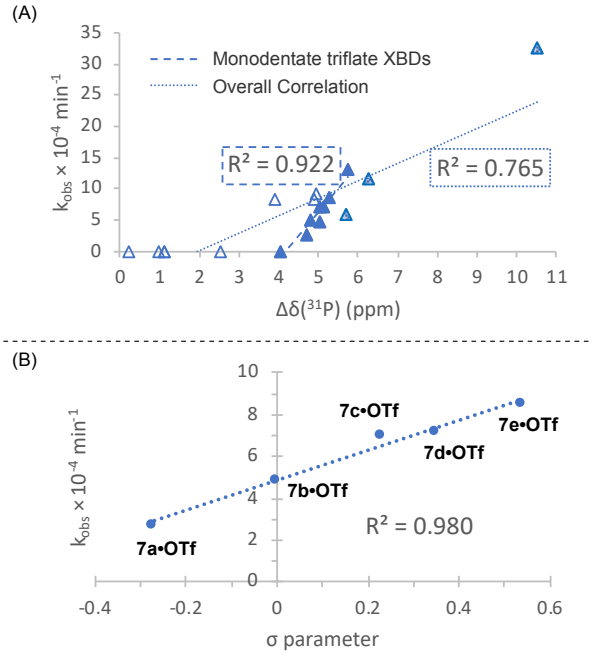

Figure 7. (A) Relationship between $\Delta\delta(^{31}P)$ and k_{obs} (Table 1) for the Friedel–Crafts addition reaction of indole **10** to *trans*-crotonophenone **11** in CD_2Cl_2 (▲: subset of monodentate triflate XBDs; ▲: subset of BAr^F XBDs; △: all other XBDs). (B) Correlation of Hammett σ parameters and k_{obs}.

Comparison of Δδ(³¹P) values between non-covalent interactions TEPO binding and ^{31}P NMR quantification provides a common scale to compare X-bonding with other non-covalent interactions commonly used in catalysis. X-bonding is a relatively weak non-covalent interaction with $\Delta\delta(^{31}P)$ values for TEPO binding up to 10.5 ppm compared to that of H-bonding (up to 24.6 ppm)[16] and Lewis acid-ligand/counterion complexes (up to 48.2 ppm).[15c]

Conclusions A commercially available phosphine oxide can quantify X-bonding ability using ^{31}P NMR spectroscopy. Altering the structures and halogen atoms on XBD scaffolds supports that TEPO is probing X-bonding interactions. We also demonstrated that TEPO binding serves as a sensitive indicator of residual acidic impurities. We successfully correlated $\Delta\delta(^{31}P)$ values for TEPO binding with activation free energy values previously reported for a Friedel–Crafts indole addition reaction with *trans*-crotonophenone. TEPO binding also correlated with catalytic activity measured within the class of monodentate triflate XBDs. We expect that this rapid method can be applied to predict the catalytic ability of new XBDs that will enhance knowledge for X-bonding catalysis.

ASSOCIATED CONTENT

Supporting Information

The Supporting Information is available free of charge on the ACS Publications website.

Experimental procedures, characterization, ^{31}P NMR data, NMR spectra and kinetic analysis (PDF)

AUTHOR INFORMATION

Corresponding Author

*E-mail: akfranz@ucdavis.edu.

ORCID

Annaliese K. Franz: 0000-0002-4841-2448
Yun-Pu Chang: 0000-0003-2866-1735
Teresa Tang 0000-0002-5014-1771
Jake R. Jagannathan: 0000-0002-1549-4272

Notes

The authors declare no competing financial interest.

ACKNOWLEDGMENT

We acknowledge the National Science Foundation for support of this research (CHE-1900300 and 1560479) and the UCOP-HBCU initiative for funding support of J. Brown. T. Tang acknowledges a UC Davis Provost's Undergraduate Fellowship. Mira Milic and Alma Perez are acknowledged for preliminary discussion and technical experiments performed as part of an FYS-CURE.

REFERENCES

(1) (a) Cavallo, G.; Metrangolo, P.; Milani, R.; Pilati, T.; Priimagi, A.; Resnati, G.; Terraneo, G. The Halogen Bond. *Chem. Rev.* **2016**, *116* (4), 2478–2601. (b) Desiraju, G. R.; Ho, P. S.; Kloo, L.; Legon, A. C.; Marquardt, R.; Metrangolo, P.; Politzer, P.; Resnati, G.; Rissanen, K. Definition of the Halogen Bond (IUPAC Recommendations 2013). *Pure and Applied Chemistry* **2013**, *85*, 1711–1713.

(2) (a) Berger, G.; Soubhye, J.; Meyer, F. Halogen Bonding in Polymer Science: From Crystal Engineering to Functional Supramolecular Polymers and Materials. *Polym. Chem.* **2015**, *6*, 3559–3580. Berger, G.; Soubhye, J.; Meyer, F. *Polym. Chem.* **2015**, *6*, 3559–3580. (b) Mukherjee, A.; Tothadi, S.; Desiraju, G. R. Halogen Bonds in Crystal Engineering: Like Hydrogen Bonds yet Different. *Acc. Chem. Res.* **2014**, *47*, 2514–2524. Mukherjee, A.; Tothadi, S.; Desiraju, G. R. *Acc. Chem. Res.* **2014**, *47*, 2514–2524.

(3) (a) Metrangolo, P.; Neukirch, H.; Pilati, T.; Resnati, G. Halogen Bonding Based Recognition Processes: A World Parallel to Hydrogen Bonding. *Acc. Chem. Res.* **2005**, *38*, 386–395. (b) *Halogen Bonding, Fundamentals and Applications*, ed. Mingos, D. M. P. Springer-Verlag, Berlin, 2008.

(4) (a) Scholfield, M. R.; Zanden, C. M. V.; Carter, M.; Ho, P. S. Halogen Bonding (X-Bonding): A Biological Perspective. *Protein Sci* **2013**, *22*, 139–152. (b) Metrangolo, P.; Resnati, G. CHEMISTRY: Halogen Versus Hydrogen. *Science* **2008**, *321*, 918–919.

(5) (a) Bulfield, D.; Huber, S. M. Halogen Bonding in Organic Synthesis and Organocatalysis. *Chem. Eur. J.* **2016**, *22*, 14434–14450. (b) Bamberger, J.; Ostler, F.; Mancheño, O. G. Frontiers in Halogen and Chalcogen-Bond Donor Organocatalysis. *ChemCatChem* **2019**, *11*, 5198–5211. (c) Kniep, F.; Rout, L.; Walter, S. M.; Bensch, H. K. V.; Jungbauer, S. H.; Herdtweck, E.; Huber, S. M. 5-Iodo-1,2,3-Triazolium-Based Multidentate Halogen-Bond Donors as Activating Reagents. *Chem. Commun.* **2012**, *48* (74), 9299–9301. (d) Jungbauer, S. H.; Walter, S. M.; Schindler, S.; Rout, L.; Kniep, F.; Huber, S. M. Activation of a Carbonyl Compound by Halogen Bonding. *Chem. Commun.* **2014**, *50*, 6281. (e) Jungbauer, S. H.; Huber, S. M. Cationic Multidentate Halogen-Bond Donors in Halide Abstraction Organocatalysis: Catalyst Optimization by Preorganization. *J. Am. Chem. Soc.* **2015**, *137*, 12110–12120. (f) Takeda, Y.; Hisakuni, D.; Lin, C.-H.; Minakata, S. 2-Halogenoimidazolium Salt Catalyzed Aza-Diels–Alder Reaction through Halogen-Bond Formation. *Org. Lett.* **2015**, *17*, 318–321. (g) Walter, S. M.; Kniep, F.; Herdtweck, E.; Huber, S. M. Halogen-Bond-Induced Activation of a Carbon-Heteroatom Bond. *Angew. Chem. Int. Ed.* **2011**, *50*, 7187–7191. (h) Chan, Y.-C.; Yeung, Y.-Y. Halogen Bond Catalyzed Bromocarbocyclization. *Angew. Chem. Int. Ed.* **2018**, *57*, 3483–3487. (i) Saito, M.; Tsuji, N.; Kobayashi, Y.; Takemoto, Y. Direct Dehydroxylative Coupling Reaction of Alcohols with Organosilanes through Si–X Bond Activation by Halogen Bonding. *Org. Lett.* **2015**, *17*, 3000–3003. (j) Squitieri, R. A.; Fitzpatrick, K. P.; Jaworski, A. A.; Scheidt, K. A. Synthesis and Evaluation of Azolium-Based Halogen-Bond Donors. *Chem. Eur. J.* **2019**, *25* (43), 10069–10073. (k) Liu, X.; Ma, S.; Toy, P. H. Halogen Bond-Catalyzed Friedel–Crafts Reactions of Aldehydes and Ketones Using a Bidentate Halogen Bond Donor Catalyst: Synthesis of Symmetrical Bis(Indolyl)Methanes. *Org. Lett.* **2019**, *21* (22), 9212–9216. (l) Sutar, R. L.; Huber, S. M. Catalysis of Organic Reactions through Halogen Bonding. *ACS Catal.* **2019**, *9* (10), 9622–9639. (6) Erdélyi, M. Halogen Bonding in Solution. *Chem. Soc. Rev.* **2012**, *41*, 3547–3557.

(7) (a) Beale, T. M.; Chudzinski, M. G.; Sarwar, M. G.; Taylor, M. S. Halogen Bonding in Solution: Thermodynamics and Applications. *Chem. Soc. Rev.* **2013**, *42*, 1667–1680. (b) Benesi, H. A.; Hildebrand, J. H. A Spectrophotometric Investigation of the Interaction of Iodine with Aromatic Hydrocarbons. *J. Am. Chem. Soc.* **1949**, *71* (8), 2703–2707. (c) Klaboe, P. The Raman spectra of some iodine, bromine, and iodine monochloride charge-transfer coomplexes in solution *J. Am. Chem. Soc.* **1967**, *89*, 3667–3676.

(8) Laurence, C.; Queignec-Cabanetos, M.; Dziembowska, T.; Queignec, R.; Wojtkowiak, B. 1-Iodoacetylenes. 1. Spectroscopic Evidence of Their Complexes with Lewis Bases. A Spectroscopic Scale of Soft Basicity. *J. Am. Chem. Soc.* **1981**, *103* (10), 2567–2573.

(9) Fan, H.; Eliason, J. K.; Moliva A., C. D.; Olson, J. L.; Flancher, S. M.; Gealy, M. W.; Ulness, D. J. Halogen Bonding in Iodo-Perfluoroalkane/Pyridine Mixtures. *J. Phys. Chem. A* **2009**, *113* (51), 14052–14059.

(10) Wash, P. L.; Ma, S.; Obst, U.; Rebek, J. Nitrogen−Halogen Intermolecular Forces in Solution. *J. Am. Chem. Soc.* **1999**, *121* (34), 7973–7974.

(11) (a) von der Heiden, D.; Vanderkooy, A.; Erdélyi, M. Halogen Bonding in Solution: NMR Spectroscopic Approaches. *Coordination Chemistry Reviews* **2020**, *407*, 213147. (b) Sarwar, M. G.; Dragisic, B.; Salsberg, L. J.; Gouliaras, C.; Taylor, M. S. Thermodynamics of Halogen Bonding in Solution: Substituent, Structural, and Solvent Effects. *J. Am. Chem. Soc.* **2010**, *132*, 1646–1653. (c) Metrangolo, P.; Panzeri, W.; Recupero, F.; Resnati, G. Perfluorocarbon−hydrocarbon Self-Assembly Part 16. ^{19}F NMR Study of the Halogen Bonding between Halo-Perfluorocarbons and Heteroatom Containing Hydrocarbons. *J. Fluorine Chem.* **2002**, 27−33.

(12) (a) Rege, P. D.; Malkina, O. L.; Goroff, N. S. The Effect of Lewis Bases on the ^{13} C NMR of Iodoalkynes. *J. Am. Chem. Soc.* **2002**, *124*, 370–371. (b) Glaser, R.; Chen, N.; Wu, H.; Knotts, N.; Kaupp, M. ^{13}C NMR Study of Halogen Bonding of Haloarenes: Measurements of Solvent Effects and Theoretical Analysis. *J. Am. Chem. Soc.* **2004**, *126*, 4412–4419.

(13) Hakkert, S. B.; Gräfenstein, J.; Erdelyi, M. The ^{15}N NMR Chemical Shift in the Characterization of Weak Halogen Bonding in Solution. *Faraday Discuss.* **2017**, *203*, 333–346.

(14) (a) Mayer, U.; Gutmann, V.; Gerger, W. The Acceptor Number–A Quantitative Empirical Parameter for the Electrophilic Properties of Solvents *Monatsh. Chem.* **1975**, *106*, 1235−1257. (b) Beckett, M. A.; Strickland, G. C.; Holland, J. R.; Sukumar Varma, K. A Convenient n.m.r. Method for the Measurement of Lewis Acidity at Boron Centres: Correlation of Reaction Rates of Lewis Acid Initiated Epoxide Polymerizations with Lewis Acidity. *Polymer* **1996**, *37*, 4629–4631.

(15) (a) Nödling, A. R.; Müther, K.; Rohde, V. H. G.; Hilt, G.; Oestreich, M. Ferrocene-Stabilized Silicon Cations as Caalysts for Diels–Alder Reactions: Attempted Experimental Quantification of Lewis Acidity and ReactIR Kinetic Analysis. *Organometallics* **2014**, *33* (1), 302–308. (b) Nödling, A. R.; Jakab, G.; Schreiner, P. R.; Hilt, G. ^{31}P NMR Sectroscopically Quantified Hydrogen-Bonding Strength of Thioureas and Their Catalytic Activity in Diels–Alder Reactions. *Eur. J. Org. Chem.* **2014**, *2014* (29), 6394–6398. (c) Jennings, J. J.; Wigman, B. W.; Armstrong, B. M.; Franz, A. K. NMR Quantification of the Effects of Ligands and Counterions on Lewis Acid Catalysis. *J. Org. Chem.* **2019**, *84* (24), 15845–15853. (d) Jagannathan, J. R.; Diemoz, K. M.; Targos, K.; Fettinger, J. C.; Franz, A. K. Kinetic and Binding Studies Reveal Cooperativity and Off-Cycle Competition for H-Bonding Catalysis with Silsesquioxane Silanols. *Chem. Eur. J.* **2019**, *25* (65), 14953–14958.

(16) Diemoz, K. M.; Franz, A. K. NMR Quantification of Hydrogen-Bond-Activating Effects for Organocatalysts Including Boronic Acids. *J. Org. Chem* **2019**, *84*, 1126–1138.

(17) Walter, S. M.; Kniep, F.; Rout, L.; Schmidtchen, F. P.; Herdtweck, E.; Huber, S. M. Isothermal Calorimetric Titrations on Charge-Assisted Halogen Bonds: Role of Entropy, Counterions, Solvent, and Temperature. *J. Am. Chem. Soc.* **2012**, *134*, 8507–8512.

(18) To obtain valid and reproducible numbers, it is important to ensure that no residual triflic acid is present, which can lead to large $\Delta\delta(^{31}P)$ values due to TfOH−TEPO binding.

(19) When different probes such as d-pyridine and tetraethyl methylenebis(phosphonate) were evaluated, no obvious changes in chemical shift were observed. Using chlorodiethylphosphine was not evaluated as a probe because it is a highly flammable liquid. TEPO was determined to be the most safe, stable and effective phosphorous probe relative to other options.

(20) Job plots were performed and confirmed a 1:1 binding stoichiometry with TEPO for both **6•OTf** and **8c•OTf** (see Supporting Information, Section IV).

(21) Preliminary calculations of binding constants (K_a) based on data from titration experiments: **6•OTf,** $K_a = 50 \pm 4$ M^{-1}, **8c•OTf**, $K_a = 15 \pm 3$ M^{-1}, and **8c•BAr^F,** $K_a = 186 \pm 4$ M^{-1}. See Supporting Information (Section III) for more details.

(22) The larger $\Delta\delta(^{31}P)$ value of **5a•OTf** also removes the potential for TEPO-binding to be attributed to H-bonding interaction with C4 and C5 protons on the cationic imidazolium core.

(23) Krossing, I.; Raabe, I. Noncoordinating Anions—Fact or Fiction? A Survey of Likely Candidates. *Angew. Chem. Int. Ed.* **2004**, *43* (16), 2066–2090.

(24) For the discussion of counter-anion series, see details in Supporting Information (Section VId).

(25) For bis(imidazolium) triflates, the Job plot demonstrates a 1:1 binding pattern for **8c•OTf** with TEPO and $\Delta\delta(^{31}P) = 4.95$ ppm. Furthermore, the $\Delta\delta(^{31}P)$ values of mono-iodinated **8b•OTf** (4.88 ppm) and di-iodinated **8c•OTf** (4.95 ppm) are comparable, suggesting that the steric interactions of the meta-substituted bis(imidazolium) triflate do not favor bidentate X-bonding interactions with TEPO.

(26) Due to the low solubility of para-substituted bis(imidazolium) **9•OTf**, $\Delta\delta(^{31}P)$ was collected using 3 equiv of XBD.

(27) For the effect of residual TfOH on $\Delta\delta(^{31}P)$ values and the examination of purification procedure for XBD triflates, see details in Supporting Information, Section VIa.

(28) von der Heiden, D.; Detmar, E.; Kuchta, R.; Breugst, M. Activation of Michael Acceptors by Halogen-Bond Donors. *Synlett* **2018**, *29*, 1307–1313.

(29) Gliese, J.-P.; Jungbauer, S. H.; Huber, S. M. A Halogen-Bonding-Catalyzed Michael Addition Reaction. *Chem. Commun.* **2017**, *53*, 12052–12055.

(30) Molecular iodine has been reported as a catalyst in this reaction, see: von der Heiden, D.; Bozkus, S.; Klussmann, M.; Breugst, M. Reaction Mechanism of Iodine-Catalyzed Michael Additions. *J. Org. Chem.* **2017**, *82* (8), 4037–4043. The investigation of $\Delta\delta(^{31}P)$ values and the catalytic activity of molecular iodine was also attempted here (see Supporting Information, Section VIf). We observed varied NMR signals and believe that HI and/or higher iodine species are involved under TEPO binding conditions which led us not to include these $\Delta\delta(^{31}P)$ values in the correlation.

(31) Induction periods were observed in kinetic experiments which are attributed to the dissociation of XBD salts to produce the active forms of the catalyst during the induction period (see reference 28 and details in Section VIIIb of Supporting Information).